BIOCHEMISTRY
including biophysical chemistry & molecular biology

Article

pubs.acs.org/biochemistry

Flavin–Protein Complexes: Aromatic Stacking Assisted by a Hydrogen Bond

Djemel Hamdane,*[,†] Charles Bou-Nader,[†] David Cornu,[‡] Gaston Hui-Bon-Hoa,[§] and Marc Fontecave[†]

[†]Laboratoire de Chimie des Processus Biologiques, CNRS-UMR 8229, Collège De France, France 11 place Marcelin Berthelot, 75231 Paris Cedex 05, France

[‡]INSERM U779, 78 Rue du Général Leclerc, 94275 Le Kremlin-Bicêtre, France

[§]Plateforme IMAGIF, Centre de Recherche de Gif, Centre National de la Recherche Scientifique, 1 avenue de le terrasse, 91191 Gif Sur Yvette, France

Supporting Information

ABSTRACT: Enzyme-catalyzed reactions often rely on a noncovalently bound cofactor whose reactivity is tuned by its immediate environment. Flavin cofactors, the most versatile catalyst encountered in biology, are often maintained within the protein throughout numbers of complex ionic and aromatic interactions. Here, we have investigated the role of $\pi-\pi$ stacking and hydrogen bond interactions between a tyrosine and the isoalloxazine moiety of the flavin adenine dinucleotide (FAD) in an FAD-dependent RNA methyltransferase. Combining several static and time-resolved spectroscopies as well as biochemical approaches, we showed that aromatic stacking is assisted by a hydrogen bond between the phenol group and the amide of an adjacent active site loop. A mechanism of recognition and binding of the redox cofactor is proposed.

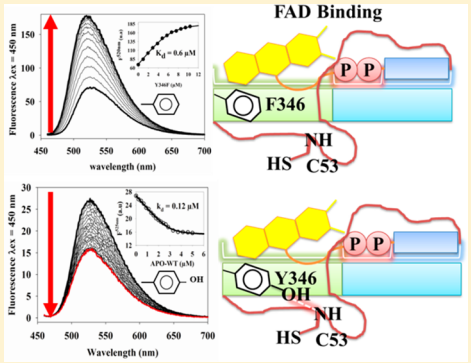

Many biological reactions are catalyzed by cofactor-dependent enzymes. For this purpose, these enzymes have to recognize their specific cofactor, bind it, and finally stabilize it within the catalytic site in a proper orientation for catalysis. Besides metal ions, a number of small organic biomolecules are used as cofactors. Flavins such as flavin mononucleotide (FMN) and flavin adenine dinucleotide (FAD) are the most versatile organic cofactors in living cells. The large chemical diversity of flavin-dependent reactions encompasses dehydrogenation, oxidation, monooxygenation, halogenation, reduction of disulfides and various types of double bond, and sensing processes (e.g., light and redox status).[1−8] Over the past several years, there have been exciting developments in the field of flavoenzymology, with the discovery of new flavoenzymes that are unexpectedly implicated in biological processes such as protein folding, apoptosis, axon guidance, chromatin remodeling, and nucleotide biosynthesis.[9,10] The wide range of processes catalyzed by flavoenzymes makes them promising leads for chemical synthetic catalysts.[11] In this context, it is crucial to better understand the molecular basis for such versatility and in particular the link between flavin reactivity and its binding mode. Flavin binds to the enzyme's active site mostly through noncovalent interactions. Among them, aromatic stacking interactions are particularly important because they provide an efficient method of molecular recognition and allow fine modulation of the redox reactivity of the flavin.[11−18] Crystal structures of several flavoenzymes have revealed that stacking often involves an aromatic residue of the protein (such as phenylalanine, tyrosine side chains) and the isoalloxazine ring of the flavin.[19−22] FMN-containing flavodoxins, for example, have been exquisite models for investigating the reversible association between the protein and FMN because they are small, abundant, stable proteins and the cofactor interacts noncovalently throughout ionic and aromatic interactions.[23−26] Furthermore, FMN is less complex than FAD, which has an additional 5′-adenosine monophosphate (5′-AMP) moiety (Figure 1A). Nevertheless, the mechanism of FMN recognition and binding by the apoprotein remains partly unclear. Indeed, the pathway(s) by which the FMN cofactor binds to the apoprotein has been the subject of several debates. Notably, there has been some disagreement regarding the location of the initial interaction between the FMN and the apoprotein as well as the degree of conformational change associated with this interaction.[27−33] The situation is even more unclear in the case of FAD, while it is the flavin cofactor most employed by flavoenzymes. We have recently characterized the complex chemical mechanism of an FAD-dependent RNA methyltransferase (TrmFO) that catalyzes the formation of 5-methyluridine at position 54 in tRNAs.[34−37] The enzyme transfers a methylene moiety from the initial carbon donor, the methylenetetrahydrofolate (CH_2THF), to the nucleophilic N^5 atom of the fully reduced $FADH^-$ forming a highly reactive

Received: May 6, 2015
Revised: June 22, 2015
Published: June 29, 2015

DOI: 10.1021/acs.biochem.5b00501
Biochemistry 2015, 54, 4354−4364

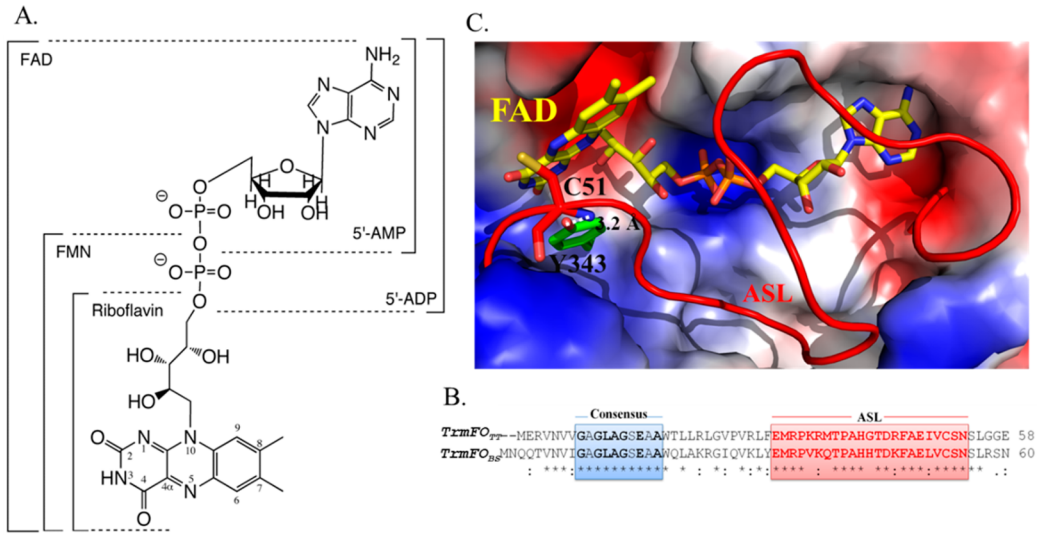

Figure 1. (A) Chemical structure of FAD and its constituting moieties. (B) Sequence alignment of the N-terminal regions of $TrmFO_{TT}$ and $TrmFO_{BS}$. The flavoproteins are classified by a consensus sequence containing the amino acid side implicated in the binding of the ribose diphosphate of FAD. The consensus sequence of the TrmFO family is delimited by a blue box and is shared by the glutathione reductase. The sequence and the boundaries of $TrmFO_{TT}$ and $TrmFO_{BS}$ ASL are delimited by the red box. (C) Electrostatic surface (±5 kT/e, red for negative and blue for positive) of the $TrmFO_{TT}$ FAD binding site. The FAD molecule is represented as yellow sticks. The 5′-ADP of the FAD moiety is completely wrapped by the N-terminal region of the ASL, whereas the isoalloxazine is stacked against the phenol group of the conserved Y343 (green). The OH group of the side chain of Y346 is poised 3.2 Å from the NH amide of the conserved C51 (red).

iminium intermediate.[36,37] The activated methylene is subsequently transferred to the tRNA, and the electrons stored in $FADH^-$ serve to reduce the exocyclic methylene into a methyl group. The ability of FAD to cycle between several redox and alkylated forms is unique in flavoenzymology, and this reactivity must be finely tuned by its protein environment. The crystal structure of TrmFO from *Thermus thermophilus* ($TrmFO_{TT}$) allowed the identification of several important amino acids in the immediate proximity of FAD.[38] The adenosine, pyrophosphate, and ribityl moieties of FAD make extensive interactions with the NH amide group of several amino acids within the consensus sequence (Figure 1B). The *si* face of the isoalloxazine ring is held by the side chains of extremely conserved cysteine 51 (C51) and tyrosine 343 (Y343) residues through van der Waals interactions, while the *re* face is accessible to the solvent for catalysis (Figure 1C). Y343 is engaged in a $\pi-\pi$ stacking interaction with the pyrimidine moiety of the isoalloxazine, and its amide group establishes a hydrogen bond with the O2 atom of the flavin ring. Moreover, its hydroxyl group makes a hydrogen bond with the NH amide group of C51 located in a long flexible active site loop (ASL) lining along the isoalloxazine edge and covering the ADP moiety of FAD (Figure 1C). Under these circumstances, we thought that this particular residue deserved a more detailed characterization. For the study reported here, we choose TrmFO from *Bacillus subtilis* ($TrmFO_{BS}$) in which the cysteine and tyrosine residues corresponding to C51 and Y343 are located at positions 53 (C53) and 346 (Y346), respectively. Our results establish that the hydrogen bond between the hydroxyl of Y346 and the amide chain of the important C53 allows the productive $\pi-\pi$ aromatic interaction. We also propose for the first time a mechanism of recognition and binding of the FAD redox cofactor by the apoprotein likely shared by most noncovalent FAD-containing proteins.

MATERIALS AND METHODS

Protein Preparations. Wild-type holo-$TrmFO_{BS}$ was expressed and purified as previously described.[39] Y346A and Y346F mutants were prepared by site-directed mutagenesis using the QuikChange site-directed mutagenesis kit (Stratagene). The mutants were expressed and purified as described for the wild-type enzyme. Briefly, the C-terminally His_6-tagged Y346 mutants were expressed in *Escherichia coli* BL21(DE3) in LB medium. The cells were grown in the dark at 37 °C until the OD_{600} was 0.6 and then induced with 0.5 mM isopropyl 1-thio-β-D-galactopyranoside (IPTG). After overnight incubation at 29 °C, the cells were harvested by centrifugation at 3000*g* for 15 min at 4 °C and the resulting pellets were resuspended in 50 mM sodium phosphate (pH 8), 300 mM NaCl, and 20 mM imidazole (buffer A) containing 20 μL of Protein Inhibitor Cocktail (PIC, Sigma) and 5 mM β-mercaptoethanol. The cells were lysed by sonication, and the lysate was centrifuged at 3000*g* for 40 min. The supernatants were subsequently loaded at 4 °C onto a 5 mL Ni^{2+}-NTA agarose affinity column (Qiagen) pre-equilibrated with buffer A. After being washed with 5 column volumes of buffer A, the mutants were eluted with buffer A containing 250 mM imidazole. The proteins were further purified on a HighLoad 16/60 Superdex 200 column equilibrated in 50 mM sodium phosphate (pH 8) and 150 mM NaCl. The fractions containing the Y346 mutant were pooled, and their purity was judged by SDS−PAGE. The protein concentration was determined by the Bradford method. After purification, all the proteins were concentrated and stored in 50 mM sodium phosphate (pH 8), 150 mM NaCl, and 20% (v/v) glycerol and stored at −80 °C. If necessary, the buffer was exchanged on a PD10 column (GE healthcare). The amount of purified protein obtained from 1 L of LB was estimated to be ∼30 and 15 mg for Y346A and Y346F mutants, respectively. The quality of the protein mutants was checked by analytical gel filtration on a Superdex 200 10/300 GL instrument (GE healthcare) and by dynamic light scattering using a Zetasier

DOI: 10.1021/acs.biochem.5b00501
Biochemistry 2015, 54, 4354−4364

Nano-ZSP (Malvern). Both techniques indicated that the samples were homogeneous and that both Y346A and Y346F variants were purified as stable monomers. For preparation of wild-type apoprotein, holo-TrmFO (30 mg/mL) in 3 mL was dialyzed for 9 days against six changes of 500 mL of 2 M KBr in 50 mM sodium phosphate (pH 9) containing 300 μM EDTA and 5 mM DTT. The protein aggregates were removed by centrifugation at 10000*g* and 4 °C for 15 min. The supernatant containing ∼1 mg of protein was recovered and exchanged with 50 mM sodium phosphate (pH 8), 150 mM NaCl, and 20% (v/v) glycerol on a PD10 column. Because we noticed that freezing the apoprotein impeded FAD binding, the protein was always used just after its preparation.

Gel Shift Assay. Protein−tRNA complexes with holo-TrmFO, Y346A TrmFO, and Y346F TrmFO were reconstituted in vitro by mixing 10 μM bulk tRNA purified form *Bacillus subtilis* strain BFS2838 carrying inactivated the *gidΩerm*^{R} gene with increasing amounts of protein (from 4 to 136 μM) in 50 mM *N*-(2-hydroxyethyl)piperazine-*N*-2-ethanesulfonic acid-Na buffer (HEPES-Na, Sigma) (pH 7.5), 100 mM ammonium sulfate, 100 μM EDTA, 25 mM mercaptoethanol (Promega), and 20% glycerol (buffer A) to a final volume of 20 μL. Bulk tRNAs of *B. subtilis* BFS2838 were obtained essentially as described previously,[40] except that the tRNA deacylation step was omitted. The samples were incubated for 20 min at 25 °C, and then 1% bromophenol blue was added to the mixture. The samples were loaded on native gel acrylamide/Bis (37.5:1), and electrophoresis was conducted for 2 h at 4 °C and 100 V. RNAs were colored with a 0.1% toluidine solution.

Test of Methylation of tRNA. The kinetics of formation of m5U54 by TrmFO was determined as described previously using an *E. coli* [α-^{32}P]UTP-labeled tRNA^{Asp} transcript.[34−36] The reaction was started by the addition of 0.2 μM holo-TrmFO or freshly purified Y346 mutants. The reaction was stopped at different incubation times by the addition of phenol. After extraction of the radioactive transcript, the tRNA was subjected to nuclease P1 (Roche), which generated 5′-nucleoside monophosphates. The various hydrolysates were then analyzed by two-dimensional thin-layer chromatography on cellulose plates (Machery Nagel). The amount of m^{5}U formed per tRNA molecule was determined by measuring the radioactivity in the TLC spots using a PhosphorImager screen and quantification with ImageQuant.

Probing the Ability of TrmFO$_{BS}$ To Form a Covalent Complex with 5-FU MiniRNA. The 5-FU mini-RNA used was 5′P-GGUCCGGGCGGG(5-FU)UCGAGUCCCGUCC-GGACC-OH3′ (Thermo Fisher Scientific Dharmacon) and corresponds to nucleotides 1−7 and 50−72 of *B. subtilis* tRNA^{Asp}. The same mini-RNA without the 5-F had been shown to be a substrate of TrmFO$_{BS}$.[35] The lyophilized mini-RNA was dissolved in RNase free water to a final concentration of 1 mM. Prior to being mixed with the protein, the 5-FU-containing mini-RNA was refolded by being heated at 80 °C for 5 min and then cooled on ice for 2 min. To probe the formation of a covalent TrmFO$_{BS}$−RNA complex, the holoprotein, Y346A mutant, or Y346F mutant at a final concentration of ∼30 μM was incubated at 37 °C for 40 min with a 2-fold molar excess of 5-FU mini-RNA in buffer A. The covalent RNA−enzyme complex was visualized on a 12% SDS−PAGE gel stained with Coomassie blue.

Fluorescence Assay. The emission fluorescence spectra of FAD alone and in complex with the proteins were recorded in a quartz cuvette at room temperature on a Cary eclipse fluorescence spectrophotometer (Varian). The excitation and emission slits were set at 5 and 10 nm, respectively. After excitation at 450 nm, the fluorescence emission was recorded every nanometer from 460 to 700 nm. The resulting spectra were corrected from the contribution of the buffer [50 mM sodium phosphate (pH 8.0)]. In all experiments, the concentration of FAD was 2 or 5 μM while that of proteins was varied. Before the spectra were recorded, protein and FAD were incubated for 5 min to reach the equilibrium. The dissociation constant (K_d) of the protein−FAD complex was determined by fitting the fluorescence emission at 525 nm to eq 1 as previously described:[31]

$$F = F_{end} + F_\delta\left[\frac{C_F - (C_A + K_d + C_F) - \sqrt{(C_A + K_d + C_F)^2 - 4C_AC_F}}{2}\right] \quad (1)$$

where F represents the fluorescence emission intensity at 530 nm after each addition, F_{end} is the remaining emission intensity at the end of the titration, F_δ is the difference in emission intensity between 1 μM free FAD and 1 μM flavodoxin, C_A is the total protein concentration after each addition (apo + holo), K_d is the dissociation constant of the apoprotein−FAD complex in micromolar, and C_F is the starting concentration of flavin.

The kinetics of FAD replacement from the apoprotein−FAD complex by ADP were measured by the fluorescence emission of flavin at 520 nm. Briefly, FAD (2 μM) was incubated with wild-type apoprotein or mutants (∼10 μM) for 5 min. Then, the FAD replacement started after the addition of ADP (2 mM).

With notations of A (apoTrmFO), B (ADP), and C (FAD), and considering A and B in excess relative to C to treat the association as a pseudo-first-order reaction, the overall rate (λ) for the replacement reaction depends on both the individual association and dissociation rates:

$$\lambda = (k_{off}^{AC}k_{on}^{AB}[B])/(k_{on}^{AB}[B] + k_{on}^{AC}[C]) \text{ if } [B] \gg [C]$$

Therefore, the observed replacement rate is $\lambda \sim k_{off}^{AC}$.

Stopped-Flow Kinetics. The binding kinetics of FAD were performed on a TGK Scientific SF-61DX2 stopped-flow fluorescence spectrophotometer equipped with a temperature-controlled circulating water bath. FAD (1 μM) was rapidly mixed with various protein concentrations. All reactions were performed in reaction buffer [50 mM sodium phosphate (pH 8.0)] at 20 °C. FAD fluorescence was recorded by exciting at 450 nm and collected through a GG-455 nm cutoff filter. Up to three transients were collected and averaged for each condition. The background signal was determined against buffer to allow data scaling. The observed rates (k_{on}) were determined by fitting the averaged transients to a single-exponential equation (eq 2) using SigmaPlot 12.

$$\Delta F = A\ \exp(-k_{on}t) \quad (2)$$

Circular Dichroism and Thermal Stability. Circular dichroism spectra were recorded with a Chirascan-plus CD spectrometer (Applied Photophysics). The protein samples were in 5 mM phosphate buffer (pH 7.5). The far-ultraviolet spectra (190−260 nm) were measured in quartz cells with an optical path length of of 0.5 or 4 mm and represent an average of four accumulations. Spectra were acquired at a resolution of

DOI: 10.1021/acs.biochem.5b00501
Biochemistry 2015, 54, 4354−4364

1 nm, with time per points set to 1 s and a bandwidth of 1 nm. All spectra were corrected for the buffer baseline. The proteins were subjected to the thermal melting profile by monitoring the changes in circular dichroism spectra from 195 to 250 nm. For thermal unfolding curves from 25 to 70 °C, samples were continuously scanned at a rate of 0.5 °C min^{-1}. The bandwidth was set to 1 nm, and the time per points was set to 0.7 s. The protein samples were in 5 mM sodium phosphate buffer (pH 7.5) in a 4/10 mm quartz cuvette. The thermal denaturation curves were analyzed with a simple two-state model for folded (N) and unfolded (U) protein: curves for the circular dichroism signal (Y_{obs}) as a function of temperature (T) were fitted using a nonlinear least-squares analysis to the following equation (eq 3):

$$Y_{obs} = \frac{Y_N + m_N T + (Y_U + m_U T)\exp\left[\frac{\Delta H_m}{R}\left(\frac{1}{T} - \frac{1}{T_m}\right)\right]}{1 + \exp\left[\frac{\Delta H_m}{R}\left(\frac{1}{T} - \frac{1}{T_m}\right)\right]} \quad (3)$$

where Y_{obs} represents the observed circular dichroism signal, Y_N and Y_U are the spectral parameters of the native (with slope m_N) and denatured (with slope m_U) forms, respectively, T is the temperature, R is the gas constant (8.314 J K^{-1} mol^{-1}), ΔH_m is the apparent van't Hoff enthalpy, and T_m is the apparent temperature of transition (i.e., 50% of the protein is in the native state).

Fluorescence Measurements under High Pressure. High-pressure experiments were conducted using a 5 mm × 5 mm quartz cuvette contained within a high-pressure cell and surrounded by a copper jacket for temperature control. The sample compartments of the SLM 8000 spectrofluorometer were modified to accept the high-pressure system, which has four sapphire windows for both transmission and 90° fluorescence studies.[41] The tryptophans of $TrmFO_{BS}$ protein at a final concentration of ~35 μM were excited at 295 nm (8 nm slits), and the emission was monitored from 310 to 450 nm (4 nm slits). No photobleaching was observed under our experimental conditions. Following each pressure increment, the enzyme was allowed to equilibrate for at least 5 min before fluorescence emission was recorded. The standard volume change during unfolding, ΔV^0, at temperature T was determined from the simulation of the equation $\Delta V^0 = [\partial \Delta G^0(p)/\partial p]_T$, where $\Delta G^0(p)$ is the standard Gibbs free energy change at pressure p, determined from the equilibrium constant for a two-state transition model, $\Delta G^0(p) = -RT \ln K_{eq} = -RT \ln[(F_N - F_p)/(F_p - F_D)]$, where F_p is the fluorescence intensity at pressure p and F_N and F_D are the asymptotic intensity values of the native and denatured states, respectively. The standard Gibbs free energy change at 0.1 MPa is obtained according to the equation $\Delta G^0 = \lim \Delta G^0(p)$ when $p \rightarrow 0.1$ MPa. The half-transition pressure ($P_{1/2}$) is given by the equation $P_{1/2} = -\Delta G^0/\Delta V^0$.

Limited Proteolysis and Mass Spectrometry Analysis. The mild trypsinolysis was conducted with 3.5 μg of $TrmFO_{BS}$ (~4 μM) with a 1/200 mass ratio of trypsin (pancreatic bovine; Sigma) for different times at room temperature in 20 μL of 50 mM HEPES (pH 7.5) containing 100 mM ammonium acetate, 200 μM EDTA, 1 mM mercaptoethanol, and 20% glycerol. The proteolysis reactions were stopped by the addition of the serine protease inhibitor 4-(2-aminoethyl)-benzenesulfonyl fluoride (Perfabloc SC, Euromedex) at a final concentration of 0.5 mM and heated in loading buffer for 2 min at 90 °C. For the experiments in the presence of FAD, the wild-type apoprotein or the Y346A or Y346F mutant (~4 μM) was incubated with 40 μM FAD for 15 min prior to trypsin treatment. Digested protein (7.5 μg) was loaded on a 12% SDS−polyacrylamide gel and analyzed by Coomassie blue staining. Bands corresponding to TrmFO proteins were excised and subjected to enzymatic digestion. Briefly, protein bands were excised and extensively washed with CH_3CN and 25 mM NH_4HCO_3. The excised bands were treated with 100 μL of 10 mM DTT at 57 °C for 30 min. The DTT was removed, and 100 μL of 55 mM iodoacetamide was added for cysteine carbamidomethylation. The reaction was allowed to proceed at room temperature for 30 min. After removal of the supernatant, the gel slices were washed again with CH_3CN and 25 mM NH_4HCO_3 and dried. We added 20 μL of 10 ng/μL Asp-N (Roche) diluted in 25 mM NH_4HCO_3, and the mixture was incubated overnight at room temperature. Peptides were extracted in 60% acetonitrile and 0.1% (v/v) formic acid, and 0.5 μL was mixed with an equal volume of α-cyano-4-hydroxycinnamic acid [10 mg/mL, 50% CH_3CN (Sigma-Aldrich)]. Crystals were obtained using the dried droplet method, and AspN-generated peptide mixtures were analyzed by MALDI-TOF-TOF 5800 (ABSciex). Survey scans were performed using delayed extraction (390 ns) in reflector mode for a total of 15000 shots. Peak lists were processed and analyzed with ProteinPilot software (ABSciex), using the MASCOT algorithm. The search parameters were as follows: $TrmFO_{BS}$ sequence, digest reagent Asp-N (cleavage at the N-terminus of D/E) or semitrypsin, cysteine carbamidomethylation, and oxidation (methionine and tryptophan) were considered a complete and variable modification, and the peptide mass tolerance was set at 10 ppm.

RESULTS AND DISCUSSION

A molecular model of $TrmFO_{BS}$ confirmed that Y346 is engaged in the same interactions as those observed in $TrmFO_{TT}$ (Figure S1 and discussion of the Supporting Information). Therefore, to evaluate the role of Y346 in the binding of FAD, two mutants, Y346F and Y346A, were generated. The Y346F mutant is expected to conserve the ability to stack against the isoalloxazine ring, while it should lose the ability to engage in a hydrogen bond with the NH amide group of C53. In contrast, the alanine variant is expected to abolish both interactions. Replacement of the tyrosine with either an alanine or a phenylalanine did not modify significantly the secondary structure of the wild-type protein as evidenced by the similar far-UV circular dichroism of Y346F, Y346A, and wild type holo-TrmFO (Figure S2 of the Supporting Information).

Characterization of the Optical Properties of the Tyrosine 346 Mutants. UV−visible spectroscopy was used to verify the presence of FAD in the mutants. As previously shown, wild-type holo-TrmFO exhibited a complex spectrum because of the presence of three enzyme populations[36,37] (Figure S3A of the Supporting Information). One contains a noncovalently bound oxidized FAD (FAD_{ox}), while the second contains a reduced FAD covalently attached via a methylene bridge between N5 and the sulfur atom of a C53. This latter species is endowed with a tRNA methylating activity from now termed a methylating species (MS). The third population contains a catalytically inactive radical derived from the former by a one-electron oxidation (Figure S3A of the Supporting Information). These spectral features disappeared upon C53 mutation, which generates a protein containing only FAD_{ox}

DOI: 10.1021/acs.biochem.5b00501
Biochemistry 2015, 54, 4354−4364

(Figure S3A of the Supporting Information). In contrast to wild-type holo-TrmFO and the C53A mutant, the visible spectrum of both Y346 variants did not contain FAD_{ox} features while they displayed a broad band at ~355 nm attributed exclusively to MS, present in only ~7 and <4% of Y346A and Y346F proteins, respectively (Figure S3A of the Supporting Information). Y346 mutants were thus purified mainly as an apoprotein form. Obviously, FAD binding has been greatly affected by the deletion of the phenol group at position 346. A phenylalanine in this position could not replace the tyrosine, and it was slightly more deleterious than an alanine. Several changes in the absorbance spectra of free FAD_{ox} were observed upon addition of either Y346 mutant, which is consistent with the binding of the flavin to the apoprotein (Figure S3B,C of the Supporting Information). Furthermore, in these reconstituted holoprotein Y346F and Y346A mutants, the maximal peak of their major flavin absorbance S0−S1 transition in the 450 nm region has been red-shifted by 2 and 7 nm relative to the C53A holo-TrmFO (~445 nm) (Figure S3 of the Supporting Information), demonstrating that the polarity of the native environment of the isoalloxazine has been altered by the mutations.

Tyrosine 346 Is Not Required for tRNA Binding, Covalent Catalysis, or Methylation. To determine whether the mutants retained the ability of the protein to bind tRNAs, the freshly purified variants were subjected to a gel shift assay with bulk tRNAs isolated from a *B. subtilis* strain deleted from TrmFO and compared with that performed in the presence of wild-type holoprotein. Mutation of Y346 did not significantly impair the capacity of TrmFO to form a stable complex with the tRNA (Figure 2A), showing that FAD is not required for tRNA recognition or binding. It has been established that following the binding of tRNA, the wild-type holoenzyme has to flip out U54 into the active site and activate the C5 position of uridine by addition of C226 cysteinate of the protein to the C6 position of the uridine, thus generating a covalent intermediate complex between TrmFO and the tRNA substrate.[35,38] This complex is formed irreversibly when the RNA substrate contains a 5-fluorouridine at the target position.[35] Similarly, the formation of a covalent complex was scrutinized in the Y346 mutants by using a 31-mer *B. subtilis* mini-$tRNA^{Asp}$ containing 5-fluorouridine at the target position (5-FU mini-RNA). In the case of wild-type holo-TrmFO, the covalent complex appears on a SDS electrophoresis gel as a well-defined band corresponding to a species migrating more slowly than the free enzyme (Figure 2B). The same phenomenon was observed in the case of Y346 mutants (Figure 2B). Finally, as shown in Figure 2C, Y346 mutants were active for methylation of a tRNA transcript with formation of m^5U54 at a rate comparable to that of the wild type (Figure 2C). Altogether, the results firmly establish that tyrosine 346 is not required for (i) binding the tRNA substrate properly, (ii) forming the FAD-based methylating agent, and (iii) the later being active during tRNA methylation. The function of this tyrosine is rather restricted to FAD binding and/or its stabilization very specifically.

Tyrosine 346 Controls the Affinity of the Enzyme for the Oxidized FAD. To estimate the relative importance of stacking and hydrogen bond properties of Y346, the affinity of both mutants for FAD_{ox} was determined by fluorescence titration. The isoalloxazine moiety is a fluorescent species that is usually quenched when bound to proteins. This spectroscopic property is used advantageously to determine K_d values for

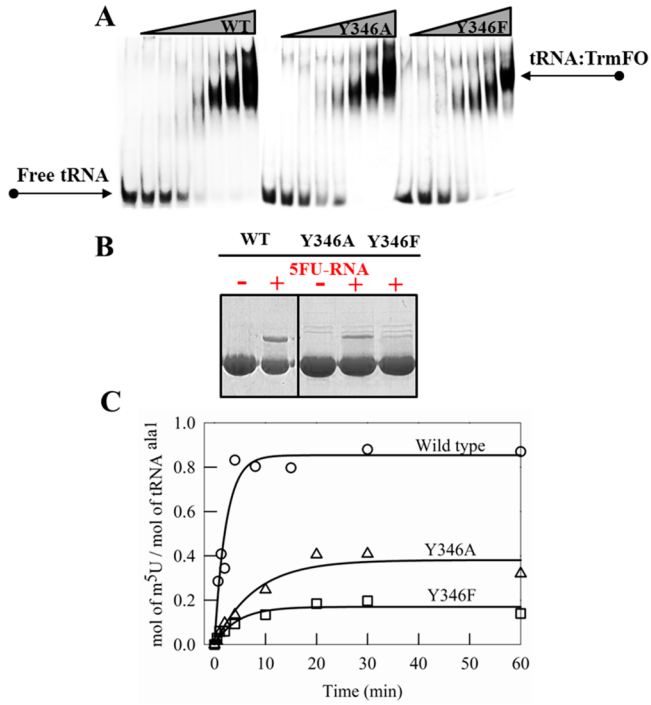

Figure 2. (A) Gel shift assays of wild-type holo-TrmFO and the as-purified Y346 mutants with bulk tRNAs. The first lane contains tRNA (10 μM) in the absence of protein, while the following lanes correspond to the tRNA (10 μM) mixed with increasing amounts of protein (2.12, 4.25, 8.5, 17, 34, 68, and 136 μM). (B) SDS−PAGE gel after Coomassie blue staining showing the formation of a covalent complex between either wild-type holoprotein or Y346 TrmFO mutants and the 5-FU-mini-RNA. (C) Time course for the tRNA m^5U54 methylation activity of $TrmFO_{BS}$. All the reactions were monitored as described in Materials and Methods. The [α-^{32}P]UTP-labeled $tRNA^{Asp}$ transcript was incubated at 37 °C under aerobic conditions with 0.2 μM freshly purified TrmFO and the reaction stopped at different times. The relative amount of m^5U formed per tRNA molecule was determined by autoradiography. Note that the activity must be conducted with freshly purified protein; otherwise, no activity was detected. Addition of free FAD (10 μM) to the Y346 mutants did not affect their kinetics of tRNA methylation. Although the wild-type apoprotein was able to bind the tRNA properly, the protein was inactive most likely because of the loss of the MS during the KBr treatment.

flavin. Surprisingly, titration of free FAD_{ox} by the Y346A or Y346F mutant resulted in an increase in flavin fluorescence (Figure 3A,B). Free FAD_{ox} in a water solution exhibits a relatively weak fluorescence quantum yield (ΦFAD ~ 0.03 vs ΦFMN ~ 0.3) as a consequence of its ADP moiety acting as an intrinsic quencher of isoalloxazine fluorescence.[42,43] On the basis of this quenching mechanism and molecular dynamic, the existence of three different FAD_{ox} conformations were identified in water, stacked, unstacked, and a partially stacked conformation, with the dominant one being the stacked conformation having the lowest fluorescence yield.[44−46] The increase in FAD_{ox} fluorescence in the presence of mutants is a clear indication that the protein has converted most of the stacked free FAD_{ox} into a protein-bound open conformation, which is not quenched by its protein environment. This contrasts with our previous denaturation experiments of wild-type TrmFO showing that the fluorescence of FAD is quenched in the holoprotein.[34−37] To resolve this discrepancy and to determine if Y346 is involved in this quenching, the wild-type

DOI: 10.1021/acs.biochem.5b00501
Biochemistry 2015, 54, 4354−4364

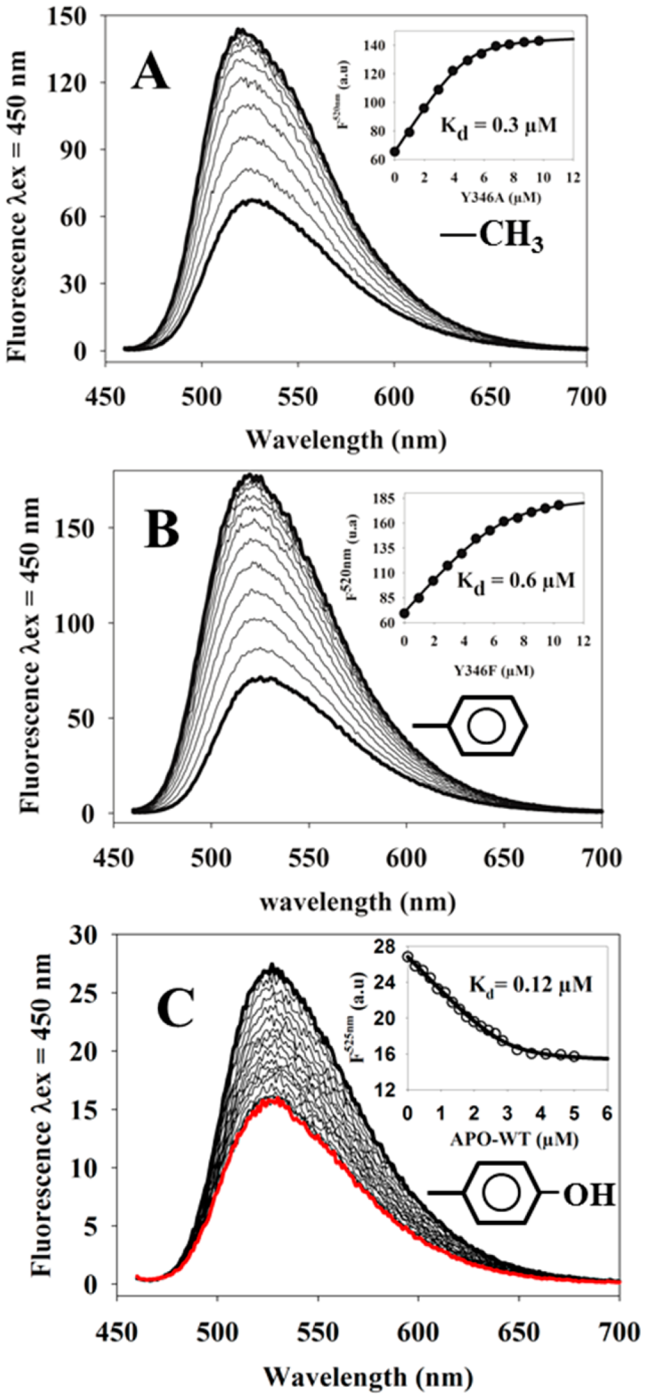

Figure 3. Fluorescence emission spectra of FAD in the presence of increasing concentrations of (A) Y346A, (B) Y346F, and (C) wild-type apoprotein in 50 mM sodium phosphate (pH 8). With the mutants, the fluorescence increased following addition of protein with a concomitant 525 to 520 nm blue shift. The insets are the variations of maximal fluorescence vs the concentration of added protein fitted to a one-binding site equation (eq 1). The dissociation constants of FAD for wild-type, Y346A, and Y346F TrmFO were 0.12 ± 0.02, 0.3 ± 0.06, and 0.6 ± 0.1, respectively.

aproprotein has been prepared from holo-TrmFO by KBr treatment and the resulting apo-TrmFO was subjected to the same fluorescence titration experiments. The KBr treatment did not disrupt the native fold of apo-TrmFO as evidenced by its far-UV circular dichroism spectrum closely resembling that of the holoprotein (Figure S2A of the Supporting Information). In contrast to both mutants, the experiments conducted with wild-type apo-TrmFO led to a decrease in FAD_{ox} fluorescence down to a plateau for around the equivalence (Figure 3C), indicating an efficient fluorescence quenching of the FAD_{ox} open conformation most likely caused by the stacking of tyrosine 346 against the isoalloxazine. Because in the mutants the isoalloxazine is not stacked, one can conclude that the hydrogen bond between the Y346 and the NH amide group of C53 is required for productive $\pi-\pi$ stacking interaction between the phenol group and the isoalloxazine moiety. We cannot discard the fact that the dipole moment of Y346 might be equally important as it is known from model studies that the phenolic ring has an affinity for stacking with the flavin ring higher than that of the phenyl ring or phenylalanine.[11] Indeed, the absence of stacking results in a decrease in the affinity of the protein for FAD by factors of ∼3 and ∼6 for Y346A and Y346F mutants, respectively (Figure 3). A phenylalanine in this position could thus not replace the tyrosine but is even more destabilizing than an alanine.

Tyrosine 346 Mutants Accelerate the Rate of FAD Dissociation. The lower affinity of Y346 variants for FAD_{ox} could originate from impairment of the rates of association or dissociation or both. To address this question, we first tried to identify the components of FAD_{ox} that are critical for recognition and binding by the apoprotein. First, we observed that the fluorescence of riboflavin or FMN was not significantly altered by the apoprotein, indicating that the isoalloxazine and the ribityl phosphate are not the major contributors for FAD binding (Figure S4 of the Supporting Information). To test whether the 5′-AMP moiety is the crucial anchoring point of the cofactor into the protein, a competition test between AMP and FAD_{ox} was performed. Addition of a large excess of 5′-AMP did not change the fluorescence of the reconstituted apoprotein−FAD complex, indicating that 5′-AMP could not displace the FAD. In contrast, a large excess of 5′-ADP led to a full dissociation of the bound FAD from the wild type and Y346 variants, confirming 5′-ADP as the major anchoring element (Figure S5 of the Supporting Information). Recently, it was shown that ADP competes with FAD in putrescine oxidase, and the enzyme was isolated with ADP bound at the ADP binding site of FAD.[47] If ADP is added at a sufficiently high concentration to the reconstituted apoprotein−FAD complex, the rate of ADP incorporation should be limited by the FAD dissociation rate. We used this approach to determine the FAD_{ox} dissociation rate constants. FAD was thus shown to be released slowly with rate constants of ∼0.018 ± 0.002, 0.01 ± 0.002, and 0.002 ± 0.0005 s^{-1} for Y346F, Y346A, and wild-type apoprotein, respectively (Figure 4A). The highest dissociation rate constants observed with the mutants are likely the major contributing factors in their lower affinity for FAD_{ox}. Finally, the kinetics of binding of FAD to Y346 variants were investigated by stopped-flow spectrofluorometry at various protein concentrations. After FAD had been rapidly mixed with the protein, the kinetics of the fluorescence increase were fitted to a monoexponential (Figure 4B). The rate constant varied linearly with the protein concentration, allowing us to calculate the bimolecular rate constant of FAD association. This rate constant for the three proteins is comparable, varying between 0.02 and ∼0.03 μM^{-1} s^{-1}. For the Y346F mutant, the linear plot intersects the observed rate constant axis at a value of ∼0.025 ± 0.003 s^{-1}, which is the k_{off} value for FAD and is consistent with that obtained from the competition reaction

DOI: 10.1021/acs.biochem.5b00501
Biochemistry 2015, 54, 4354−4364

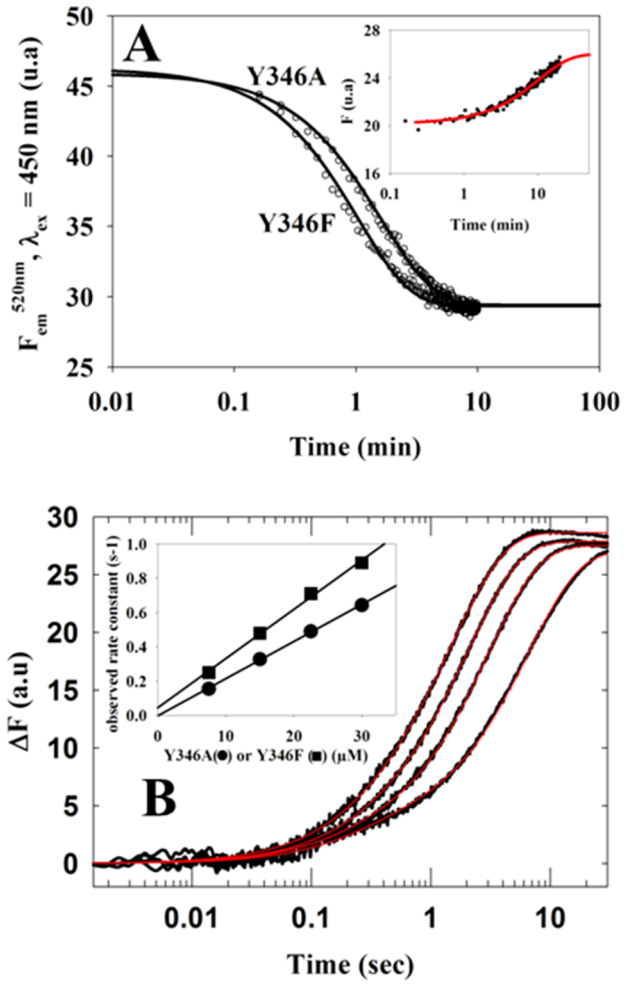

Figure 4. (A) Kinetics of dissociation of FAD from the reconstituted apoprotein−FAD complex. The kinetics corresponding to wild-type TrmFO is shown in the inset. In the Y346 mutants, the dissociation of FAD is reflected by the decrease in fluorescence at 520 nm, while for the wild type, it provokes an increase in fluorescence. The kinetics were fitted to a single exponential. (B) Kinetics of binding of FAD to Y346 mutants under pseudo-first-order conditions in 50 mM sodium phosphate (pH 8). The inset shows the observed rate constants for FAD binding as a function of protein concentration.

(Figure 4A,B). $MgCl_2$ and inorganic phosphate had no significant effect on the association rates unless they are present at a high concentration (Figure S6 of the Supporting Information). Therefore, mutations of Y346 have specifically impaired the protein−FAD complex stability, and the presence of phenylalanine endowed with a stacking capability is not enough to decrease the dissociation rate constant of the redox cofactor.

Conformational Stability of the Tyrosine Mutants. The presence of a redox cofactor often stabilizes the native protein.[26]To investigate the effect of Y346 on the conformational stability of the protein, the structural changes induced by high pressure were monitored through tryptophan fluorescence spectroscopy. Conformational changes ultimately leading to unfolding can be induced by increased pressure.[48−52] Increasing the hydrostatic pressure provoked a sigmoidal augmentation of fluorescence for wild-type holoprotein and as-isolated TrmFO mutants (Figure S7 of the Supporting Information). The transition observed with wild-type holo-TrmFO was characterized by a volume change (ΔV_0) of -75.8 ± 3 cm^3 mol^{-1} and a half-transition pressure $P_{1/2}$ of ~156 ± 9 MPa. Replacement of Y346 with either an alanine or a phenylalanine leads to lower $P_{1/2}$ values (108 ± 7 and 95 ± 4 MPa for Y346A and Y346F, respectively), reflecting decreased protein stability. The Y346F mutation is a more destabilizing mutation, which is also corroborated by thermal denaturation experiments (Figure S8 of the Supporting Information). Furthermore, apparent ΔV_0 values increased upon Y346 mutation (-83 ± 3 and -97 ± 5 cm^3 mol^{-1} for Y346A and Y346F, respectively). As previously suggested, this is an indication of a reduction in the size of internal cavities and of an increased penetration of water molecules into the protein core.[53] In the mutants, the absence of FAD may have exposed hydrophobic pockets forced to be filled by water under high pressure. To further substantiate this hypothesis, the ability of the holoprotein and the Y346 variants to bind ANS had been measured. ANS is a fluorescent probe of accessible hydrophobic patches, and its binding to solvent-accessible clusters of nonpolar side chains leads to a marked increase in fluorescence emission accompanied by a blue shift. The binding of ANS to holo-TrmFO provoked a significant increase of the ANS fluorescence with a blue shift (Figure S9 of the Supporting Information). As for the Y346 mutants, the amplitude and the blue-shift of the maximal peak of ANS fluorescence were more pronounced, indicating that the absence of FAD exposes hydrophobic regions that are protected by the FAD in the holoenzyme (Figure S9 of the Supporting Information). Hence, FAD is important for the overall stability of the protein most likely by ordering the flexibility around the active site.

Ordering the Active Site Loop by the FAD Cofactor. Proteases are known to cut at flexible and accessible polypeptide sites, and limited trypsinolysis can be used to assess the mobility of loops that are adjacent to redox cofactors. We have used this strategy to evaluate the impact of the mutations and FAD binding on the structure of the active site loop (ASL) lining along the isoalloxazine that is connected to Y346 by a hydrogen bond with C53 (Figure 1C). Wild-type apo-TrmFO and Y346 mutants were thus subjected to mild trypsinolysis treatments either in the absence or in the presence of an excess of FAD (Figure 5). The results showed that all trypsin-treated proteins were cleaved to different extents, generating a fragment that migrated on the gel at a position corresponding to a mass of ~45 kDa. Cleavage was shown to occur at R59 by mass spectrometry and peptide mass fingerprinting analysis, generating a truncated form named Δ59-TrmFO (Figure S10 of the Supporting Information). Interestingly, we observed that FAD had a strong protecting effect on the wild-type protein (Figure 5A), as no Δ59-TrmFO was detected after reaction for more than 2 h. Hence, while in the wild-type apoprotein R59 seems to be accessible to trypsin, in the holoprotein this site becomes buried, which is consistent with the structural model of holo-$TrmFO_{BS}$ (Figure S6 of the Supporting Information). Likewise, the binding of FAD to wild-type apoprotein has efficiently ordered the conformational sampling of the ASL in the vicinity of the R59. In contrast, in the case of both mutants, FAD protected from proteolysis only partly, pointing to the critical function of Y346, and more specifically the H-bond between Y346 and C53, for controlling the structural flexibility of the loop and protecting R59 from trypsinolysis (Figure 5). As shown from the fluorescence studies (Figure S4 of the Supporting Information), ADP is primordial for the firm binding of FAD to the apoprotein. To

DOI: 10.1021/acs.biochem.5b00501
Biochemistry 2015, 54, 4354−4364

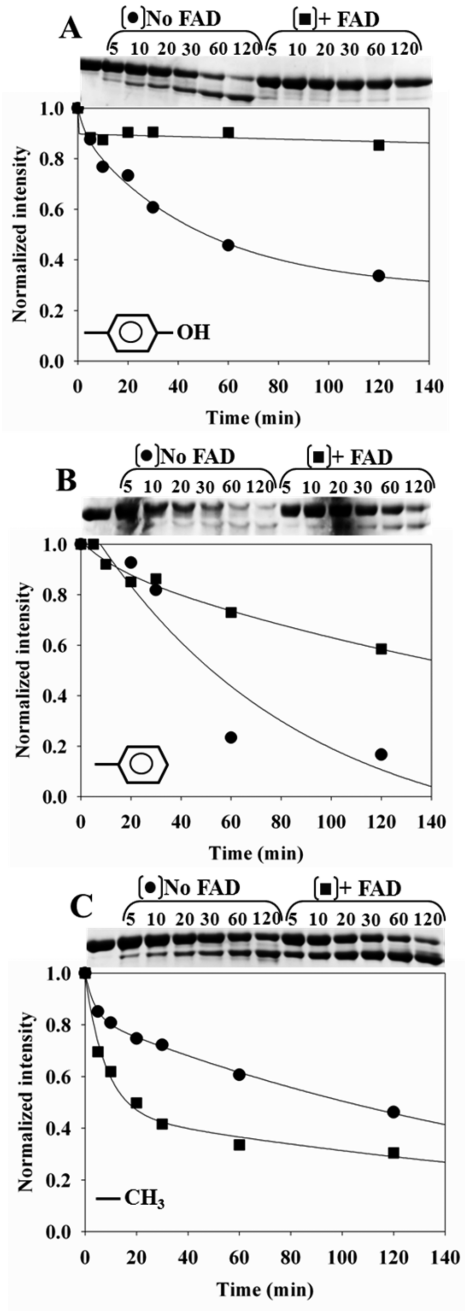

Figure 5. Limited proteolytic profiles in the absence and presence of FAD for (A) wild-type apoprotein, (B) Y346F, and (C) Y346A TrmFO. The mild trypsinolysis kinetics were conducted with the incubation of ~4 μM protein and a 1/200 mass ratio of trypsin for different times and stopped by the addition of the serine protease inhibitor 4-(2-aminoethyl)benzenesulfonyl fluoride (Perfabloc SC, Euromedex). For the experiments in the presence of FAD, the wild-type apoprotein or the Y346A or -F mutant (~4 μM) was incubated with 40 μM FAD for 15 min prior to trypsin treatment. Digested protein (7.5 μg) was loaded on a 12% SDS–polyacrylamide gel and analyzed by Coomassie blue staining.

test if the ADP binding to wild-type apoprotein could protect the protein from trypsin cleavage, the mild trypsinolysis was repeated in the presence of ADP. The ADP-bound TrmFO was as sensitive as the wild -type apoprotein to trypsin treatment (data not shown), indicating that the protecting effect of FAD is likely caused by the binding of isoalloxazine, which is located ~7 Å from R59 (Figure 6).

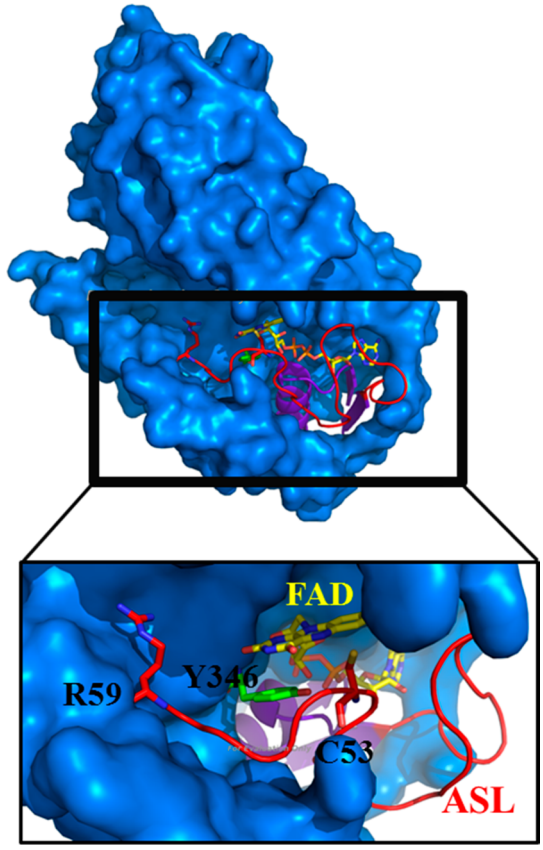

Figure 6. Surface representation of a $TrmFO_{BS}$ homology model with a close-up on the FAD finding site. The ASL is colored red, and R59 determined to be the cleavage site of tryprin is represented as sticks.

CONCLUSION

Altogether, the results presented here establish that the hydrogen bond between the hydroxyl group of Y346 and the NH amide group of C53 favors a productive stacking between the tyrosine and the isoalloxazine ring of FAD. First, the purified Y346F mutant, in which the phenylalanine should conserve the ability to stack against the isoalloxazine, contains less FAD than the Y346A mutant. Second, the quenching of FAD fluorescence by the apoprotein is observed only with the wild type and not with Y346F mutant, indicating that in the latter, the phenylalanine does not stack properly against the isoalloxazine ring of FAD. Third, the Y346F mutant exhibits an affinity for FAD ~2 and ~6 times lower than that for Y346A and wild-type apoprotein, respectively. According to the kinetic data, this difference is mainly attributed to its higher FAD dissociation rate constant. Fourth, FAD plays a major role in the structure and conformational flexibility of the ASL, which is not the case for the Y346F mutant. For all these reasons, it appears that in Y346F mutant, the phenylalanine is not engaged in a productive $\pi-\pi$ stacking interaction with the isoalloxazine.

On the basis of all our results, a mechanism of FAD recognition and binding can be postulated (Figure 7). First, reversible binding of FAD by TrmFO is an indication that the redox cofactor is incorporated into a folded state of the protein. In aqueous medium, FAD coexists under several reversible

DOI: 10.1021/acs.biochem.5b00501
Biochemistry 2015, 54, 4354–4364

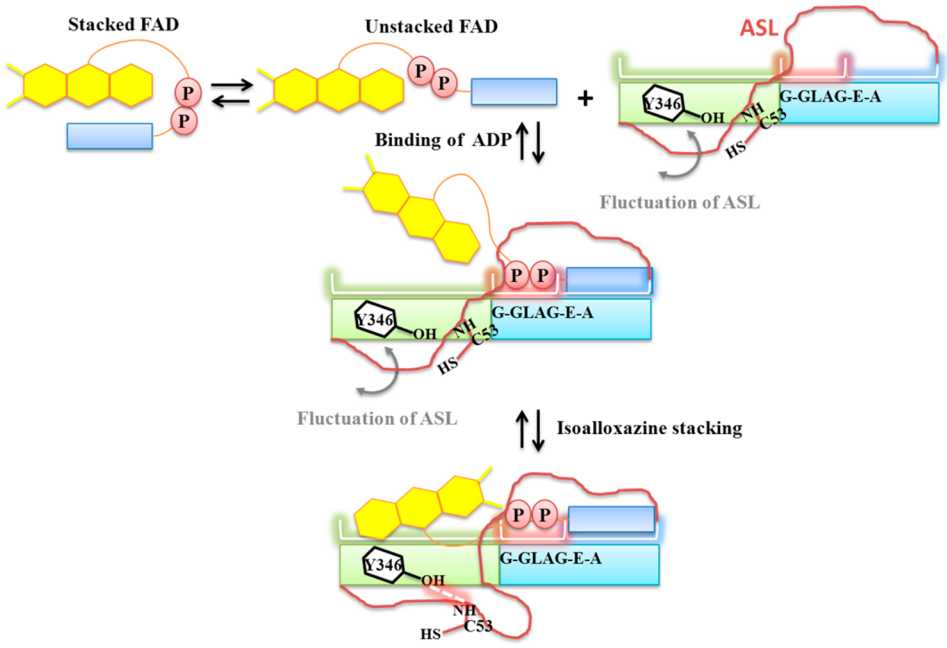

Figure 7. Proposed mechanism of FAD recognition and binding by the apoprotein.

conformations; nonetheless, the closed conformation in which the isoalloxazine stacked against the adenine moiety is the predominant form.[44−46] The apoprotein displaces the equilibrium toward the unstacked form of FAD by anchoring the 5′-ADP moiety throughout interaction with several amino acids of the consensus sequence located in the positively charged groove of the FAD binding site. The use of the ADP moiety as the major anchoring point to the apoprotein has been observed in several flavoenzymes,[47,54,55] and this phenomenon could be a general feature among the FAD binding proteins. Anchoring the ADP likely restricts the conformational sampling of the cofactor and may help the isoalloxazine to translocate into the active site. As soon as the isoalloxazine binds, the mobility of the ASL is diminished and the H-bond between the OH group of Y346 and the NH amide of C53 stabilizes the phenol side chain from free rotation. This reinforces the $\pi-\pi$ overlap and consequently orders the FAD binding in the most compact and energetically favorable state for catalysis. The proposed bipartite binding mechanism of FAD is reminiscent of that of another dinucleotide redox cofactor, the NAD(P)H.[56,57] By anchoring the adenosine ribophosphate moiety to the enzyme, the nicotinamide moiety of NAD(P)H is free to explore the accessible conformational space until reaching the proper configuration for hydride transfer. This shared binding mechanism may be partly due to the presence of the same canonical dinucleotide binding motif carried by the Rossman fold. The conformational sampling mechanism is widespread in biological electron transfer systems[58] and could be at the origin of redox cofactor binding specificity.

■ ASSOCIATED CONTENT

Supporting Information

Far-UV CD and UV−visible absorption spectra, fluorescence spectra of riboflavin and FMN in the presence of apoprotein, fluorescence spectra of the FAD-reconstituted Y346 mutants in the presence of ADP, variation of the FAD association rate constant with inorganic phosphate or $MgCl_2$, pressure and thermal denaturation curves, binding of ANS to TrmFO, and mass spectrometry characterization of Δ59-TrmFO. The Supporting Information is available free of charge on the ACS Publications website at DOI: 10.1021/acs.biochem.5b00501.

■ AUTHOR INFORMATION

Corresponding Author

*Laboratoire de Chimie des Processus Biologiques, CNRS-UMR 8229, Collège De France, France 11 place Marcelin Berthelot, 75231 Paris Cedex 05, France. Telephone: +00-331-44 27 12 78. E-mail: djemel.hamdane@college-de-france.fr.

Funding

This work was supported by the Centre National de la Recherche Scientifique, the Fondation de l'Orangerie for individual Philanthropy and its donors, and the French State Program "Investissements d'Avenir" (Grants "LABEX DYNAMO", ANR-11-LABX-0011, and IDEX Sorbonne Universités ANR-11-IDEX-0004-02 to D.H.).

Notes

The authors declare no competing financial interest.

■ ABBREVIATIONS

ADP, adenosine diphosphate; AMP, adenosine monophosphate; ANS, 8-anilinonaphthalene-1-sulfonic acid; ASL, active site loop; CD, circular dichroism; CH2THF, methylenetetrahydrofolate; FAD, flavin adenine dinucleotide; Fem, fluorescence emission; FMN, flavin mononucleotide; FU, 5-fluorouridine; λ_{ex}, excitation wavelength; m5U, 5-methyluridine; MS, methylating species; SDS−PAGE, sodium dodecyl sulfate−polyacrylamide gel electrophoresis; TrmFO, tRNA methyltransferase folate-dependent; tRNA, transfer ribonucleic acid.

■ REFERENCES

(1) Massey, V. (2000) The chemical and biological versatility of riboflavin. *Biochem. Soc. Trans. 28*, 283−296.
(2) Fraaije, M. W., and Mattevi, A. (2000) Flavoenzymes: diverse catalysts with recurrent features. *Trends Biochem. Sci. 25*, 126−132.

DOI: 10.1021/acs.biochem.5b00501
Biochemistry 2015, 54, 4354−4364

(3) Bornemann, S. (2002) Flavoenzymes that catalyse reactions with no net redox change. *Nat. Prod. Rep. 19*, 761−772.
(4) Joosten, V., and van Berkel, W. J. (2007) Flavoenzymes. *Curr. Opin. Chem. Biol. 11*, 195−202.
(5) Walsh, C. T., and Wencewicz, T. A. (2013) Flavoenzymes: versatile catalysts in biosynthetic pathways. *Nat. Prod. Rep. 30*, 175−200.
(6) Huijbers, M. M., Montersino, S., Westphal, A. H., Tischler, D., and van Berkel, W. J. (2014) Flavin dependent monooxygenases. *Arch. Biochem. Biophys. 544*, 2−17.
(7) Becker, D. F., Zhu, W., and Moxley, M. A. (2011) Flavin redox switching of protein functions. *Antioxid. Redox Signaling 14*, 1079−1091.
(8) Conrad, K. S., Manahan, C. C., and Crane, B. R. (2014) Photochemistry of flavoprotein light sensors. *Nat. Chem. Biol. 10*, 801−809.
(9) De Colibus, L., and Mattevi, A. (2006) New frontiers in structural flavoenzymology. *Curr. Opin. Struct. Biol. 16*, 722−728.
(10) Gudipati, V., Koch, K., Lienhart, W. D., and Macheroux, P. (2014) The flavoproteome of the yeast Saccharomyces cerevisiae. *Biochim. Biophys. Acta, Proteins Proteomics 1844*, 535−544.
(11) Nandwana, V., Samuel, I., Cooke, G., and Rotello, V. M. (2013) Aromatic stacking interactions in flavin model systems. *Acc. Chem. Res. 46*, 1000−1009.
(12) Gray, M., Goodman, A. J., Carroll, J. B., Bardon, K., Markey, M., Cooke, G., and Rotello, V. M. (2004) Model systems for flavoenzyme activity: interplay of hydrogen bonding and aromatic stacking in cofactor redox modulation. *Org. Lett. 6*, 385−388.
(13) Swenson, R. P., and Krey, G. D. (1994) Site-directed mutagenesis of tyrosine-98 in the flavodoxin from Desulfovibrio vulgaris (Hildenborough): regulation of oxidation-reduction properties of the bound FMN cofactor by aromatic, solvent, and electrostatic interactions. *Biochemistry 33*, 8505−8514.
(14) Zhou, Z., and Swenson, R. P. (1996) The cumulative electrostatic effect of aromatic stacking interactions and the negative electrostatic environment of the flavin mononucleotide binding site is a major determinant of the reduction potential for the flavodoxin from Desulfovibrio vulgaris [Hildenborough]. *Biochemistry 35*, 15980−15988.
(15) Lostao, A., Gómez-Moreno, C., Mayhew, S. G., and Sancho, J. (1997) Differential stabilization of the three FMN redox forms by tyrosine 94 and tryptophan 57 in flavodoxin from Anabaena and its influence on the redox potentials. *Biochemistry 36*, 14334−14344.
(16) Pellett, J. D., Becker, D. F., Saenger, A. K., Fuchs, J. A., and Stankovich, M. T. (2001) Role of aromatic stacking interactions in the modulation of the two-electron reduction potentials of flavin and substrate/product in Megasphaera elsdenii short-chain acyl-coenzyme A dehydrogenase. *Biochemistry 40*, 7720−7728.
(17) Casaus, J. L., Navarro, J. A., Hervás, M., Lostao, A., De la Rosa, M. A., Gómez-Moreno, C., Sancho, J., and Medina, M. (2002) Anabaena sp. PCC 7119 flavodoxin as electron carrier from photosystem I to ferredoxin-NADP+ reductase. Role of Trp(57) and Tyr(94). *J. Biol. Chem. 277*, 22338−22344.
(18) Kraft, B. J., Masuda, S., Kikuchi, J., Dragnea, V., Tollin, G., Zaleski, J. M., and Bauer, C. E. (2003) Spectroscopic and mutational analysis of the blue-light photoreceptor AppA: a novel photocycle involving flavin stacking with an aromatic amino acid. *Biochemistry 42*, 6726−6734.
(19) Fukuyama, K., Matsubara, H., and Rogers, L. J. (1992) Crystal structure of oxidized flavodoxin from a red alga Chondrus crispus refined at 1.8 Å resolution. Description of the flavin mononucleotide binding site. *J. Mol. Biol. 225*, 775−789.
(20) Trickey, P., Wagner, M. A., Jorns, M. S., and Mathews, F. S. (1999) Monomeric sarcosine oxidase: structure of a covalently flavinylated amine oxidizing enzyme. *Structure 7*, 331−345.
(21) Arakaki, A. K., Orellano, E. G., Calcaterra, N. B., Ottado, J., and Ceccarelli, E. A. (2001) Involvement of the flavin si-face tyrosine on the structure and function of ferredoxin-NADP+ reductases. *J. Biol. Chem. 276*, 44419−44426.
(22) Xia, C., Hamdane, D., Shen, A. L., Choi, V., Kasper, C. B., Pearl, N. M., Zhang, H., Im, S. C., Waskell, L., and Kim, J. J. (2011) Conformational changes of NADPH-cytochrome P450 oxidoreductase are essential for catalysis and cofactor binding. *J. Biol. Chem. 286*, 16246−16260.
(23) Tollin, G., and Edmondson, D. E. (1971) Chemical and physical characterization of the Shethna flavoprotein and apoprotein and kinetics and thermodynamics of flavin analog binding to the apoprotein. *Biochemistry 10*, 124−132.
(24) Mayhew, S. G. (1971) Studies on flavin binding in flavodoxins. *Biochim. Biophys. Acta 235*, 289−302.
(25) Sancho, J. (2006) Flavodoxins: sequence, folding, binding, function and beyond. *Cell. Mol. Life Sci. 63*, 855−864.
(26) Wittung-Stafshede, P. (2002) Role of cofactors in protein folding. *Acc. Chem. Res. 35*, 201−208.
(27) Genzor, C. G., Perales-Alcon, A., Sancho, J., and Romero, A. (1996) Closure of a tyrosine/tryptophan aromatic gate leads to a compact fold in apo flavodoxin. *Nat. Struct. Biol. 3*, 329−332.
(28) Steensma, E., and van Mierlo, C. P. (1998) Structural characterisation of apoflavodoxin shows that the location of the stable nucleus differs among proteins with a flavodoxin-like topology. *J. Mol. Biol. 282*, 653−666.
(29) Murray, T. A., and Swenson, R. P. (2003) Mechanism of flavin mononucleotide cofactor binding to the Desulfovibrio vulgaris flavodoxin. 1. Kinetic evidence for cooperative effects associated with the binding of inorganic phosphate and the 5′-phosphate moiety of the cofactor. *Biochemistry 42*, 2307−2316.
(30) Lostao, A., Daoudi, F., Irun, M. P., Ramon, A., Fernandez-Cabrera, C., Romero, A., and Sancho, J. (2003) How FMN binds to *Anabaena* apoflavodoxin: a hydrophobic encounter at an open binding site. *J. Biol. Chem. 278*, 24053−24061.
(31) Bollen, Y. J., Nabuurs, S. M., van Berkel, W. J., and van Mierlo, C. P. (2005) Last in, first out: the role of cofactor binding in flavodoxin folding. *J. Biol. Chem. 280*, 7836−7844.
(32) Muralidhara, B. K., Chen, M., Ma, J., and Wittung-Stafshede, P. (2005) Effect of inorganic phosphate on FMN binding and loop flexibility in *Desulfovibrio desulfuricans* apo-flavodoxin. *J. Mol. Biol. 349*, 87−97.
(33) Ayuso-Tejedor, S., Abián, O., Velázquez-Campoy, A., and Sancho, J. (2011) Mechanism of FMN Binding to the Apoflavodoxin from Helicobacter pylori. *Biochemistry 50*, 8703−8711.
(34) Hamdane, D., Guerineau, V., Un, S., and Golinelli-Pimpaneau, B. (2011) A catalytic intermediate and several flavin redox states stabilized by folate-dependent tRNA methyltransferase from *Bacillus subtilis*. *Biochemistry 50*, 5208−5219.
(35) Hamdane, D., Argentini, M., Cornu, D., Myllykallio, H., Skouloubris, S., Hui-Bon-Hoa, G., and Golinelli-Pimpaneau, B. (2011) Insights into folate/FAD-dependent tRNA methyltransferase mechanism: Role of two highly conserved cysteines in catalysis. *J. Biol. Chem. 286*, 36268−36280.
(36) Hamdane, D., Argentini, M., Cornu, D., Golinelli-Pimpaneau, B., and Fontecave, M. (2012) FAD/folate-dependent tRNA methyltransferase: Flavin as a new methyl-transfer agent. *J. Am. Chem. Soc. 134*, 19739−19745.
(37) Hamdane, D., Bruch, E., Un, S., Field, M., and Fontecave, M. (2013) Activation of a unique flavin-dependent tRNA-methylating agent. *Biochemistry 52*, 8949−8956.
(38) Nishimasu, H., Ishitani, R., Yamashita, K., Iwashita, C., Hirata, A., Hori, H., and Nureki, O. (2009) Atomic structure of a folate/FAD-dependent tRNA T54 methyltransferase. *Proc. Natl. Acad. Sci. U. S. A. 106*, 8180−8185.
(39) Hamdane, D., Skouloubris, S., Myllykallio, H., and Golinelli-Pimpaneau, B. (2010) Expression and purification of untagged and histidine-tagged folate-dependent tRNA:m5U54 methyltransferase from *Bacillus subtilis*. *Protein Expression Purif. 73*, 83−89.
(40) Urbonavicius, J., Skouloubris, S., Myllykallio, H., and Grosjean, H. (2005) Identification of a novel gene encoding a flavin-dependent tRNA:m5U methyltransferase in bacteria−evolutionary implications. *Nucleic Acids Res. 33*, 3955−3964.

DOI: 10.1021/acs.biochem.5b00501
Biochemistry 2015, 54, 4354−4364

(41) Hamdane, D., Kiger, L., Hoa, G. H., Dewilde, S., Uzan, J., Burmester, T., Hankeln, T., Moens, L., and Marden, M. C. (2005) High pressure enhances hexacoordination in neuroglobin and other globins. *J. Biol. Chem. 280*, 36809−36814.
(42) Weber, J. (1950) Fluorescence of riboflavin and flavin-adenine dinucleotide. *Biochem. J. 47*, 114−121.
(43) Weber, G., Tanaka, F., Okamoto, B. Y., and Drickamer, H. G. (1974) The effect of pressure on the molecular complex of isoalloxazine and adenine. *Proc. Natl. Acad. Sci. U. S. A. 71*, 1264−1266.
(44) van den Berg, P. A. W., Feenstra, K. A., Mark, A. E., Berendsen, H. J. C., and Visser, A. J. W. G. (2002) Dynamic Conformations of Flavin Adenine Dinucleotide: Simulated Molecular Dynamics of the Flavin Cofactor Related to the Time-Resolved Fluorescence Characteristics. *J. Phys. Chem. B 106*, 8858−8869.
(45) Islam, S. D. M., Susdorf, T., Penzkofer, A., and Hegemann, P. (2003) Fluorescence Quenching of Flavin Adenine Dinucleotide in Aqueous Solution by pH Dependent Isomerisation and Photo-Induced Electron Transfer. *Chem. Phys. 295*, 137−149.
(46) Chosrowjan, H., Taniguchi, S., Mataga, N., Tanaka, F., and Visser, A. J. W. G. (2003) The Stacked Flavin Adenine Dinucleotide Conformation in Water is Fluorescent on Picosecond Timescale. *Chem. Phys. Lett. 378*, 354−358.
(47) van Hellemond, E. W., Mazon, H., Heck, A. J., van den Heuvel, R. H., Heuts, D. P., Janssen, D. B., and Fraaije, M. W. (2008) ADP competes with FAD binding in putrescine oxidase. *J. Biol. Chem. 283*, 28259−28264.
(48) Akasaka, K. (2006) Probing conformational fluctuation of proteins by pressure perturbation. *Chem. Rev. 106*, 1814−1835.
(49) Zhang, H., Kenaan, C., Hamdane, D., Hoa, G. H., and Hollenberg, P. F. (2009) Effect of conformational dynamics on substrate recognition and specificity as probed by the introduction of a de novo disulfide bond into cytochrome P450 2B1. *J. Biol. Chem. 284*, 25678−25686.
(50) Hamdane, D., Vasseur-Godbillon, C., Baudin-Creuza, V., Hoa, G. H., and Marden, M. C. (2006) Reversible hexacoordination of alpha-hemoglobin-stabilizing protein (AHSP)/alpha hemoglobin Versus pressure. Evidence for protection of the alpha-chains by their chaperone. *J. Biol. Chem. 282*, 6398−6404.
(51) Girard, E., Marchal, S., Perez, J., Finet, S., Kahn, R., Fourme, R., Marassio, G., Dhaussy, A. C., Prangé, T., Giffard, M., Dulin, F., Bonneté, F., Lange, R., Abraini, J. H., Mezouar, M., and Colloc'h, N. (2010) Structure-function perturbation and dissociation of tetrameric urate oxidase by high hydrostatic pressure. *Biophys. J. 98*, 2365−2373.
(52) Wilton, D. J., Kitahara, R., Akasaka, K., Pandya, M. J., and Williamson, M. P. (2009) Pressure-dependent structure changes in barnase on ligand binding reveal intermediate rate fluctuations. *Biophys. J. 97*, 1482−1490.
(53) Roche, J., Caro, J. A., Norberto, D. R., Barthe, P., Roumestand, C., Schlessman, J. L., Garcia, A. E., García-Moreno, B. E., and Royer, C. A. (2012) Cavities determine the pressure unfolding of proteins. *Proc. Natl. Acad. Sci. U. S. A. 109*, 6945−6950.
(54) Wille, G., Ritter, M., Weiss, M. S., König, S., Mäntele, W., and Hübner, G. (2005) The role of Val-265 for flavin adenine dinucleotide (FAD) binding in pyruvate oxidase: FTIR, kinetic, and crystallographic studies on the enzyme variant V265A. *Biochemistry 44*, 5086−5094.
(55) Sato, K., Nishina, Y., and Shiga, K. (1992) The binding of adenine nucleotides to apo-electron-transferring flavoprotein. *J. Biochem. 112*, 804−810.
(56) Pudney, C. R., Hay, S., and Scrutton, N. S. (2009) Bipartite recognition and conformational sampling mechanisms for hydride transfer from nicotinamide coenzyme to FMN in pentaerythritol tetranitrate reductase. *FEBS J. 276*, 4780−4789.
(57) Deng, Z., Aliverti, A., Zanetti, G., Arakaki, A. K., Ottado, J., Orellano, E. G., Calcaterra, N. B., Ceccarelli, E. A., Carrillo, N., and Karplus, P. A. (1999) A productive NADP+ binding mode of ferredoxin-NADP + reductase revealed by protein engineering and crystallographic studies. *Nat. Struct. Biol. 6*, 847−853.
(58) Toogood, H. S., Leys, D., and Scrutton, N. S. (2007) Dynamics driving function: new insights from electron transferring flavoproteins and partner complexes. *FEBS J. 274*, 5481−504.

DOI: 10.1021/acs.biochem.5b00501
Biochemistry 2015, 54, 4354−4364